Contribution from the Department of Chemistry and the Ames Laboratory—DOE,[1] Iowa State University, Ames, Iowa 50011

Synthesis, Characterization, and Bonding of Indium Clusters: $Na_7In_{11.8}$, a Novel Network Structure Containing *closo*-In_{16} and *nido*-In_{11} Clusters

Slavi C. Sevov and John D. Corbett*

Received November 14, 1991

Reactions of the elements in proportions near 37.3 at. % Na at ~500, 410, and then 250 °C readily produce the well-crystallized title phase. The tetragonal structure at the indium-rich limit was solved by standard single-crystal X-ray means at room temperature ($P4_2/nmc$, $Z = 12$; $a = 16.093$ (4) Å, $c = 23.384$ (8) Å; $R(F)/R_w = 3.4/3.6\%$). The network structure consists of interbonded clusters—the first example of *closo*-In_{16} icosioctahedra ($\bar{4}m2$ symmetry) that are 8-exo-bonded, 10-bonded nido icosahedra (fractional occupancy of the eleventh cluster site generates ~36% 1,3-arachno units) and four-bonded indium atoms in pairs of triangles (In_{16}:$In_{11(10)}$:In_1 = 1:4:12). Extended Hückel calculations that include significant interactions between directional nonbonding pairs on atoms in neighboring In_{16} and In_{11} units indicate $2n + 4$ skeletal electrons are necessary for each, with no nonbonding pairs on the latter, and a closed shell for 504 electrons per cell vs 507 for the refined stoichiometry. Observed properties are in good agreement; at the indium-rich limit, the phase is a poor metal (ρ_{295} ~540 μΩ-cm) with a Pauli-like paramagnetism $\chi_M = (1.7 - 1.8) \times 10^{-4}$ emu/mol after correction for core and orbital diamagnetism. The intercluster interactions appear to be closely correlated with a small region of nonstoichiometry and changes in the *c* lattice parameter. Some general factors in a diverse indium cluster chemistry are noted.

Introduction

Reduced compounds of the boron family elements have long been famous for their important and novel examples of structures and bonding. Probably the most remarkable in both historic importance and diversity of chemistry are the boron hydrides, broadly defined. Here we need to recall mainly the family of simple borane(2-) ions. These are typified by the geometrically *closo*-$B_nH_n^{2-}$ species, which require $2n + 2$ skeletal electrons according to Wade's rules, as well as nido and arachno species, which are missing one or two vertices and possess $2n + 4$ or $2n + 6$ cluster-based electrons, respectively.[2,3] The same rules have also been generalized for the "naked" Zintl ion clusters of main group elements (Bi_8^{2+}, Sn_5^{2-}, Sn_9^{4-}, etc.) in which "inert s pairs" replace those in the exo B–H bonds in the boranes.[4,5] The lower $2n + 2$ limit appears to have been a general "floor" for the electron count in such isolated clusters.

An interesting contrast is the sparcity of aluminum analogues (see refs 6 and 7). On the other hand, gallium as a post-transition element forms many binary and ternary compounds that contain gallium clusters, fused clusters, and cluster fragments.[8-11] However, virtually no isolated clusters of gallium have been found, perhaps because the charges on such units would be too high (e.g., Ga_8^{10-} and Ga_{12}^{14-} for closo analogues of $B_8H_8^{2-}$ and $B_{12}H_{12}^{2-}$, respectively). Instead, intercluster bonding is common as this formally converts the s orbital to a bonding role and reduces the cluster charge by one for each exo bond. The results are three-dimensional network structures. Unfortunately, apparent fractional occupancy of both gallium and cation positions as well as disorder complicates the understanding and interpretation of the bonding requirements of many of the gallide structures. However, some clear-cut and successful assignments have been achieved,[8,12-14] although confirmatory property measurements have generally not been obtained.

Table I. Selected Data Collection and Refinement Parameters for $Na_7In_{11.76}$

space group	$P4_2/nmc$ (No. 137)
Z	12
a, Å[a]	16.093 (4)
c, Å	23.384 (8)
V, Å^3	6056 (4)
absorp coeff (Mo Kα), cm^{-1}	133.6
transm coeff range	0.442-1.00
no. of indep obs refl; variables	1352; 153
R,[b] %	3.4
R_w,[c] %	3.6

[a] Guinier data, λ = 1.540 562 Å. [b] $R = \sum||F_o| - |F_c||/\sum|F_o|$. [c] $R_w = [\sum w(|F_o| - |F_c|)^2/\sum w(F_o)^2]^{1/2}$; $w = \sigma(F)]^{-2}$.

Knowledge of the compositions and structures of even binary alkali metal–indium phases is generally poor. We have already reported[15] that the potassium system contains the metallic phase K_8In_{11} with isolated and unprecedented hypoelectronic In_{11}^{7-} clusters and $K_{22}In_{39}$,[16] which is essentially isostructural with $Na_{21}Ga_{39}$.[9] The latter consists of a network of heavily interbonded In_{12} and In_{15} clusters. Our present results for many binary (and some ternary) compounds formed between indium and the alkali metals (A) suggest that close structural relationships between gallium and indium (E) systems may exist only for the foregoing $A_{22}E_{39}$ and the layered AE_3[17-19] and AE (NaTl-type[20]) phases. Instead, a plethora of new indium units are found in relatively well-behaved structures.

The present article reports on our first results for Na–In system, the network structure of $Na_7In_{11.8}$ (37.3 at. % Na). Subsequent articles will provide information about other specimens, the closely related network structure of $Na_{15}In_{28}$ (34.9% Na) and the isolated tetrahedral clusters in Na_2In (66.7%).[16] All of their compositions bear little relationship to those presently assigned in the phase diagram, which is largely based on thermal analysis. Here, the compound nearest Na_7In_{12} has been approximated[21] as Na_5In_8 (38.5%) or Na_2In_3 (40.0%) on the basis of different estimates of

(1) The Ames Laboratory—DOE is operated for the U. S. Department of Energy by Iowa State University under Contract W-7405-Eng-82. This research was supported by the Office of Basic Energy Sciences, Materials Sciences Division.
(2) Wade, K. *Adv. Inorg. Chem. Radiochem.* **1976**, *18*, 1.
(3) Olah, G. A., Wade, K., Williams, R. E., Eds. *Electron Deficient Boron and Carbon Clusters*; J. Wiley: New York, 1991.
(4) Corbett, J. D. *Inorg. Chem.* **1968**, *7*, 198.
(5) Corbett, J. D. *Chem. Rev.* **1985**, *85*, 383.
(6) Hiller, W.; Klinkhammer, K.-W.; Uhl, W.; Wagner, J. *Angew. Chem., Int. Ed. Engl.* **1991**, *30*, 179.
(7) Nesper, R. *Angew. Chem., Int. Ed. Engl.* **1991**, *30*, 795.
(8) Belin, C.; Ling, R. G. *J. Solid State Chem.* **1983**, *48*, 40, and references therein.
(9) Frank-Cordier, U.; Cordier, G.; Schäfer, H. *Z. Naturforsch.* **1982**, *37B*, 119, 127.
(10) Belin, C.; Charbonnel, M. *J. Solid State Chem.* **1986**, *64*, 57.
(11) Charbonnel, M.; Belin, C. *J. Solid State Chem.* **1987**, *67*, 210.
(12) Schäfer, H. *J. Solid State Chem.* **1985**, *57*, 97.
(13) Burdett, J. K.; Canadell, E. *J. Am. Chem. Soc.* **1990**, *112*, 7207.
(14) Burdett, J. K.; Canadell, E. *Inorg. Chem.* **1991**, *30*, 1991.
(15) Sevov, S. C.; Corbett, J. D. *Inorg. Chem.* **1991**, *30*, 4875.
(16) Sevov, S. C.; Corbett, J. D. To be published.
(17) Ling, R. C.; Belin, C. *Z. Anorg. Allg. Chem.* **1981**, *480*, 181.
(18) Van Vucht, J. H. N. *J. Less-Common Met.* **1985**, *108*, 163.
(19) Tschuntonow, K. A.; Yatsenko, S. P.; Hryn, Yu. N.; Yarmolyuk, Ya. P.; Orlov, A. N. *J. Less-Common Met.* **1984**, *99*, 15.
(20) Zintl, E.; Neumayr, S. *Z. Phys. Chem.* **1933**, *B20*, 270.
(21) Larose, S.; Pelton, A. D. *J. Phase Equilib.* **1991**, *12*, 371.

0020-1669/92/1331-1895$03.00/0

the melting point maximum.[22,23] Earlier evidence for a phase near Na_3In (75%) is contradictory. The system has long been known to contain the Zintl phase NaIn (50%).[20]

Experimental Section

Synthesis. All materials were handled in a N_2-filled glovebox. The surface of the indium metal (Cerac, 99.999%) was cleaned with a scalpel before use, as was the sodium (Alpha, 99.9+%, sealed under Ar). In an exploratory reaction, a mixture with 38.5 at. % Na was loaded into a tantalum tube welded at one end. (Loss of some Na on transfer is the most probable error.) The other end of the tube was then weld-sealed in a He atmosphere, the tube was placed in a fused-silica ampule, and this was sealed under high vacuum after baking.

The components were fused at 490 °C, and the mixture was then annealed at 410 °C for 3 days and at 250 °C for 5 days. (The liquidus is at ca. 440 °C for this composition.[21]) The resulting ingot was metallic in appearance and very brittle. Its powder pattern was obtained from finely ground sample mounted between pieces of cellophane tape. An Enraf-Nonius Guinier camera, Cu Kα radiation (λ = 1.540 562 Å), and NBS (NIST) silicon as an internal standard were employed for this purpose.

Structure Determination. A few platelike pieces were picked from the crushed sample, sealed in thin-walled glass capillaries, and checked by means of oscillation, Weissenberg and precession photographs for singularity, and, eventually, a space group assignment. The photographs showed a tetragonal cell with systematic absences consistent with only one possible space group—$P4_2/nmc$ (No. 137). A crystallite ca. 0.1 × 0.1 × 0.05 mm was chosen, and X-ray data were collected (two octants, $2\theta \leq 50°$) at room temperature with the aid of a Rigaku AFC6R single-crystal diffractometer together with monochromated Mo Kα radiation. A few details of the data collection and refinement are listed in Table I.

The 25 reflections found from a random search by the diffractometer were indexed with a tetragonal cell with the expected dimensions. The diffraction data confirmed the chosen space group after their correction for Lorentz and polarization effects and for absorption with the aid of the average of ψ-scans of three reflections at different θ values.

Application of direct methods[24] gave 12 positions that were (correctly) assigned to indium in the starting model. A few cycles of least-squares refinement (TEXAN[25]) and a difference Fourier synthesis revealed 11 atom positions with distances to the indium atoms that were appropriate for sodium, and these were so assigned. Refinement with isotropic thermal parameters proceeded smoothly (R = 8.5%), but this produced an unreasonably large thermal parameter for In11. However, the electron density at this position was too high to replace it by a sodium atom, and moreover, the distances from this position to the neighboring indium atoms were undoubtedly of the order of In–In distances. Consequently this position was refined as indium with partial occupancy, 63.6 (8)% in the final analysis. The occupancies of the other In atoms did not deviate from unity by more than 3% (3σ) when the Na atoms were kept fixed and, for Na, by 4–6% ($\leq 2\sigma$) when the In atoms were fixed. Therefore, these were not varied from unity in the final refinement.

The final residuals listed were obtained after anisotropic refinement of all atoms as well as variation of the multiplicity of In11. The refined composition is $Na_7In_{11.757(5)}$ (37.32 (1) at. % Na). The largest residual peaks in the final difference Fourier map were 2.6 (1.68 Å from In10) and −1.5 e/Å^3.

A powder X-ray diffraction pattern calculated for the compound based on the refined positional parameters allowed indexing of 40 lines in the observed powder pattern. The 2θ values of these and the standard Si lines afforded the lattice constants listed for $Na_7In_{11.76}$ through least-squares refinement. The powder pattern also contained weak lines from indium metal as a second phase, probably from adventitious oxidation or hydrolysis of the sample during the X-ray exposure.

Nonstoichiometry. Two reactions containing 36.8 and 41 at. % Na were subsequently carried out under the conditions described above. Both of them showed Na_7In_{12} as a major phase, but the first also contained the indium-richer $Na_{15}In_{28}$,[16] and the second had some of the sodium-richer NaIn[20] as a second phase. The lattice parameters of the Na_7In_{12-x} component in these two products should represent the limits of any range of stoichiometry. The phase on the indium-rich side had lattice parameters of a = 16.096 (2) Å, c = 23.385 (4) Å, virtually identical to those of the sample from which the structure was refined. On the other hand, the lattice at the sodium-rich side had a = 16.107 (2) Å, c = 23.286 (4) Å, a significant contraction of the c axis (0.4%, 11–18σ) while the a axis remained about the same (0.07%, 4.2σ difference).

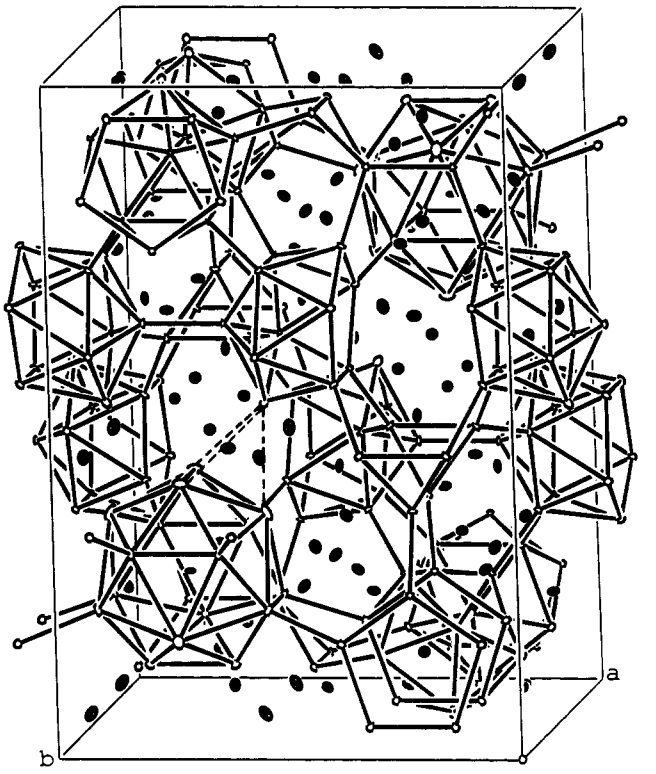

Figure 1. General view of the unit cell of $Na_7In_{11.76}$, slightly off [100] with $\vec{c}$ vertical. The In atoms are depicted as open, the Na as solid ellipsoids. Lines are drawn for all In–In separations less than 3.5 Å. One set of significant intercluster interactions between In11 in a nido icosahedron and In12 and 2In10 in the In_{16} unit is represented by dashed lines.

Electrical Resistivity. Since the compound is quite air- and moisture-sensitive, the routine four-probe method for measuring resistivity was not applicable. We used instead an electrodeless "Q" method.[26] For this purpose, the sample was ground, a fraction with an average particle diameter of 340 μm was separated, and this was mixed with an equal volume of powdered (chromatography) alumina in order to reduce contact between the sample particles. The mixture was loaded into a glass ampule and sealed under 480 Torr Ar. The Q measurements were made at 35 MHz over the temperature range of 130–295 K. A plastic bag with holes for all parts and a nest outside the coil for the thermocouple was used to avoid interference both from the thermocouple and from moisture condensation on the ampule while cooling with off-gas from liquid N_2. Readings were taken every 10 deg after waiting sufficient time to reach temperature equilibrium.

Magnetic Susceptibility. The container was constructed of fused-silica tubing (3 mm i.d.), in half of which a closely fitting silica rod had been sealed. A 25-mg sample was then loaded into the open end in the glovebox, and another such rod was inserted from the other end of the tube. The assembly was evacuated, backfilled with He, and sealed at the second end. The sample was thus fixed between the rods. This type of holder gives a very uniform background and much more reproducible results than the usual container in which the sample sits on a fused septum. The magnetization was measured at a field of 3 T over the range 6–295 K on a Quantum Design MPMS SQUID magnetometer. The raw data were corrected for the susceptibility of the container.

Results and Discussion

Structure Description. The final positional and isotropic equivalent displacement parameters and the important distances for the refined composition $Na_7In_{11.76}$ are listed in Tables II and III, respectively. The general view of the unit cell in Figure 1 outlines all In–In separations that are less than 3.5 Å. The structure can be described as a three-dimensional indium network composed of three different building blocks: a closo 16-vertex deltahedron (Figure 2a), the 11-membered nido derivative of an

(22) Lamprecht, G. J.; Crowther, P. *J. Inorg. Nucl. Chem.* **1969**, *31*, 925.
(23) Thümmel, R.; Klemm, W. *Z. Anorg. Allg. Chem.* **1970**, *376*, 44.
(24) Sheldrick, G. M. *SHELXS-86*; Universität Göttingen, BRD, 1986.
(25) *TEXAN*, Version 6.0 package; Molecular Structure Corp., The Woodlands, TX, 1990.
(26) Shinar, J.; Dehner, B.; Beaudry, B. J.; Peterson, D. T. *Phys. Rev.* **1988**, *37B*, 2066.

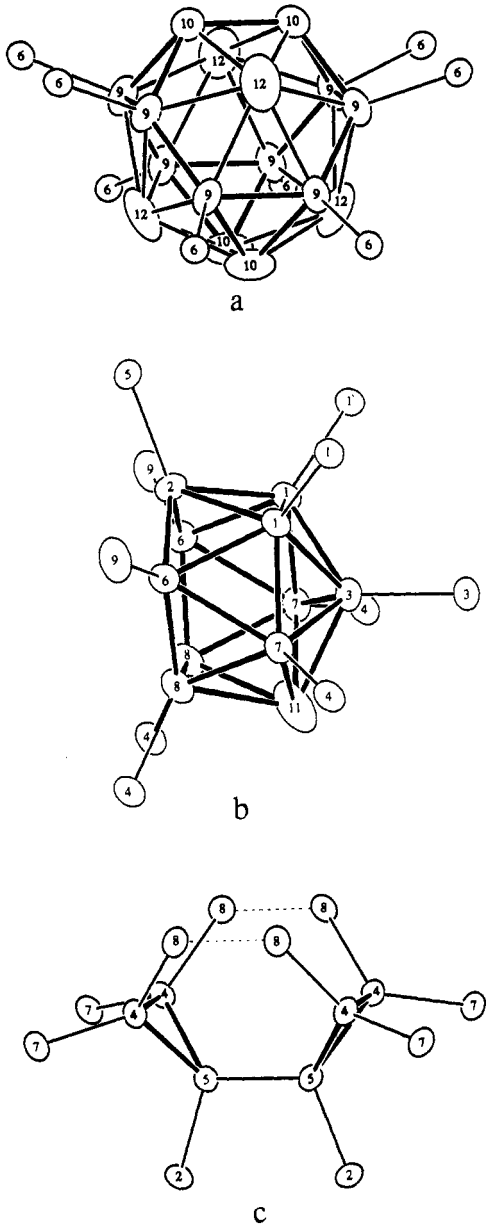

Figure 2. (a) The 16-vertex closo icosioctahedron (the centering Na^+ is not shown); (b) the nido icosahedron in which In11 is ~63.6% occupied; (c) pairs of In_3 triangles, all in $Na_7In_{11.76}$. The dangling atoms in all three represent intercluster bonds between these units (94% thermal ellipsoids).

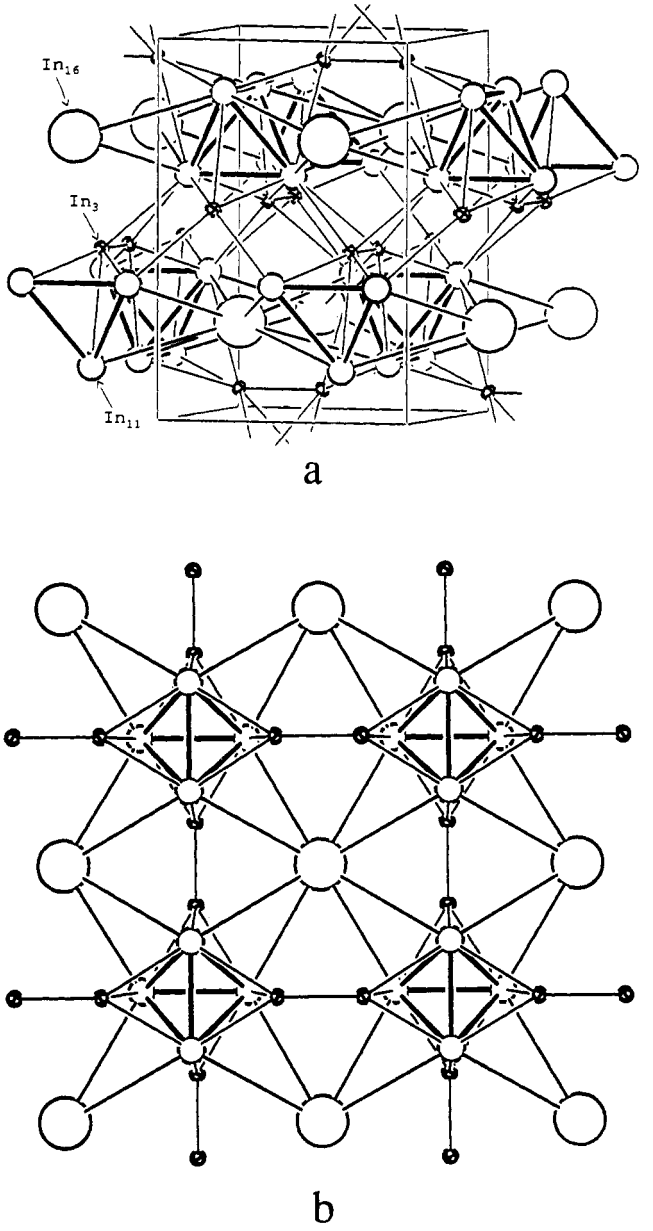

Figure 3. Representations of the layering of interbonded units in $Na_7In_{11.76}$. Large and medium circles mark the centers of In_{16} and $In_{11}(In_{10})$ clusters while small, crossed circles represent the In_3 triangles (Figure 2a–c, respectively). (a) Same orientation as Figure 1; (b) the [001] view. The $[In_{11(10)}]_4$ groups are emphasized.

icosahedron (Figure 2b), and pairs of triangles (Figure 2c). These units are 8-, 10-, and 10-bonded, respectively, to other members via exo In–In bonds that are generally somewhat shorter than those within the polyhedra.

The 16-vertex cluster (In9, -10, -12) has D_{2d} ($\bar{4}m2$) point group symmetry but is in fact very close to T_d symmetry. This polyhedron can be derived from a 12-membered truncated tetrahedron formed by In9 and In10 on which all hexagonal faces are also capped by In12. The total number of triangular faces is 28, and so it can be called an icosioctahedron (or 28-hedron). All In9 atoms therein are exo bonded to In6 in eight different icosahedra (Figure 2a and Figure 3) leaving eight atoms (In10, -12) that are members only of this polyhedron. The somewhat larger and nonuniform ellipsoids for the latter group may suggest some torsional motion (or distortion) although In12 is distinctive in that it also has longer bonds to six other indium atoms. The cluster is centered by a Na2 ion.

The nido icosahedra (In1, -2, -3, -6, -7, -8, -11) have only m symmetry and are grouped in fours about the other point of $\bar{4}m2$ symmetry (site 2 b) in this space group. All but In11 have exo bonds (Figure 2b); In1 and In3 are bonded to the same atoms in three other icosahedra, each In6 is bonded to a 16-vertex polyhedron, and In2, -7, and -8 are bonded to different In_3 triangles. The only atom without an exo bond (In11) is the one that refines as a partially occupied site (63.6%). The cluster is distorted such that In11 (when present) projects somewhat from the polyhedron. Its closest exo neighbor is In12 in In_{16} at 3.87 Å, too long to afford a strong bonding interaction between these two atoms but probably the source of some electronic effects and nonstoichiometry (below).

The third bulding block (Figure 2c) consists of pairs of triangles, each made up of two In4 atoms and one In5. These can all be considered as four-bonded, isolated In atoms. The group is bonded to eight different nido icosahedra, the dashed lines in Figure 2c between pairs of exo In8 atoms representing edges of two different icosahedra, Figure 2b.

Figure 3 shows a condensed version of the connectivity between these building blocks in two different views. Large and medium circles represent the centers of the In_{16} and In_{11} clusters, respectively, while the small crossed circles denote the positions of each of the In_3 triangles. The structure can be viewed (Figure

Table II. Positional Parameters and B_{eq} (Å^2) for $Na_7In_{11.76}$[a]

atom	posn	x	y	z	B_{eq},[b] Å^2
In1	16 *h*	0.6563 (1)	0.0659 (1)	0.29244 (6)	1.19 (6)
In2	8 *g*	1/4	0.0970 (1)	0.73247 (9)	1.2 (1)
In3	8 *g*	1/4	0.8384 (1)	0.61746 (9)	1.23 (9)
In4	16 *h*	0.8438 (1)	−0.0601 (1)	0.05747 (6)	1.29 (6)
In5	8 *g*	1/4	0.1561 (1)	0.85100 (9)	1.34 (9)
In6	16 *h*	0.5990 (1)	−0.0975 (1)	0.34123 (6)	1.41 (7)
In7	16 *h*	0.5959 (1)	0.0697 (1)	0.41476 (6)	1.31 (6)
In8	16 *h*	0.9116 (1)	−0.1581 (1)	−0.03786 (6)	1.44 (6)
In9	16 *h*	0.4331 (1)	−0.1549 (1)	0.29687 (7)	2.02 (7)
In10	8 *g*	1/4	0.8416 (2)	0.1106 (1)	3.0 (1)
In11[c]	8 *g*	1/4	0.9228 (3)	0.5016 (2)	2.8 (2)
In12	8 *g*	1/4	−0.0816 (2)	0.3361 (1)	3.8 (2)
Na1	8 *g*	1/4	0.4205 (7)	0.4056 (5)	1.9 (5)
Na2	2 *a*	3/4	1/4	3/4	1.2 (5)
Na3	2 *b*	3/4	1/4	1/4	1.8 (6)
Na4	4 *d*	1/4	1/4	0.9807 (8)	1.9 (8)
Na5	8 *g*	1/4	0.9439 (8)	0.8393 (5)	2.2 (6)
Na6	8 *g*	1/4	0.3873 (9)	0.2531 (5)	2.3 (6)
Na7	16 *h*	0.9435 (6)	−0.0583 (6)	0.1908 (4)	2.6 (4)
Na8	4 *d*	1/4	1/4	0.6294 (8)	3 (1)
Na9	16 *h*	0.0603 (6)	−0.0619 (6)	0.0600 (5)	3.4 (5)
Na10	8 *g*	1/4	0.6253 (8)	0.9791 (5)	2.2 (6)
Na11	8 *g*	1/4	0.0398 (8)	0.0764 (5)	2.2 (6)

[a] Origin at $\bar{1}$. [b] $B_{eq} = (8\pi^2/3)\sum_i\sum_j U_{ij}a_i^*a_j^*\vec{a}_i\vec{a}_j$. [c] Occupancy of 63.6 (8)%, giving the composition $Na_7In_{11.757(5)}$.

3a) as composed of macrolayers lying normal to the *c* axis. Each layer consists of squares of 16-vertex clusters, each of which is centered by a tetrahedron composed of four interconnected nido icosahedra (heavier outline), or vice versa (Figure 3b). The bonding within the layers is mainly through direct $(In_{11})_{4/4}$–$(In_{16})_{4/4}$ intercluster bonds as well as through $(In_{11})_4$–$(In_3)_2$ interactions. The different layers are held together only by the pairs of In_3 triangles or, in other words, via isolated indium atoms.

All sodium atoms except Na2, -3, and -4 cap triangular faces of the polyhedra. The same type of positioning for the alkali metal is seen in K_8In_{11}.[15] The Na2 cation is in the center of the icosioctahedron, and Na3 and Na4 center the tetrahedral holes formed by four icosahedra or three icosahedra and one triangle, respectively. The In–In distances within and between the clusters are typical for In clusters (2.84–3.06 Å) except for (a) some longer distances associated with distortion of the In_{11}, In_{10} units (3.16–3.19 Å) and (b) greater values about In12 (3.30–3.47 Å), which has six rather than five bonding neighbors within its cluster.

Properties. Resistivities of $Na_7In_{11.76}$ calculated from the Q measurements are nicely linear with temperature over 130–295 K and indicate a metallic behavior, $\rho_{295} \sim 540$ μΩ·cm with a coefficient of +0.26%/deg. Such a resistivity is characteristic of what would be termed a "poor metal". The value is logically greater than the maximum resistivity observed in liquid Na–In mixtures, $\rho_{748} \sim 180$ μΩ·cm at ~60 at. % Na.[27] (The last is close to the composition of Na_2In which contains discrete tetrahedral clusters in the solid state.[16]) It should be noted that absolute resistivities determined by the Q method are probably accurate by no more than a factor of 3, but the temperature coefficient should be quite reliable.

Magnetic measurements on $Na_7In_{11.76}$ gave temperature-independent susceptibilities of $-(5.4 - 5.5) \times 10^{-4}$ emu/mol over the range of 12–295 K. Two types of diamagnetic corrections may be subtracted from this number. The first, for the ion cores of Na^+ and In^{3+}, totals -2.6×10^{-4} emu/mol.[28] The second, a diamagnetic correction for the Larmor precession of the electron pairs in the orbitals of each cluster, can be estimated from $\chi_L = -0.79Z_i \times 10^{-6}(r_{av}/a_0)^2$ emu/mol-cluster,[29] where Z_i is the number of skeletal electrons in the cluster, r_{av} is the average radius of the orbitals (Å), and $a_0 = 0.529$ Å. For r_{av}, we appropriately averaged the distances from the center of each cluster to the middle of the different types of In–In edges on its surface. This gave 2.4 and 3.1 Å for the nido icosahedra and the icosioctahedra and, therefore, $\chi_L = -4.2 \times 10^{-4}$ and -9.8×10^{-4} emu/mol-cluster, respectively. Based on the proportions of each cluster per formula unit, the total Larmor correction per mole of Na_7In_{12} becomes $\chi_L = -(0.67 \times 4.23 + 0.17 \times 9.8) \times 10^{-4} = -4.5 \times 10^{-4}$ emu/mol. Combination of this, the ion core value, and the measured susceptibility provides $\chi_M = +(1.7 - 1.8) \times 10^{-4}$ emu/mol. This is indicative of a very small Pauli-type paramagnetism, consistent with the conductivity measured and the electron count based on theory (below). The diamagnetic corrections must be viewed as approximate; valence electrons in lone pairs and bonds between clusters and to the isolated indium atoms have not been included and will certainly increase the end result. A similar procedure has given a similar susceptibility value for K_8In_{11}, which is stoichiometric and also a poor metal.[15]

Structural Features. The most interesting aspect of this structure is the first example of the 16-vertex deltahedron. The geometry of such a cluster has been discussed before[30] in connection with the possible existence of higher order boranes. Since four six-bonded and possibly energetically less favored boron atoms would be necessary in *closo*-$B_{16}H_{16}^{2-}$, these authors proposed transition-metal-substituted analogues instead such as $(CpCo)_4B_{12}H_{12}$ or $[(OC)_3Fe]_4B_{12}H_{12}$. However, calculations suggested that a pure 16-atom boron cluster might still exist, there seeming to be a net advantage in maximizing the number of near-neighbor bonds in spite of their decreasing strengths.[31]

Here we should mention that the icosioctahedron qualifies as a closed polyhedron according to the criteria for it.[32] As far as we have been able to find in the literature, the largest *closed* clusters formed by any element in the boron group are the 15-vertex, 26-face polyhedra (icosihexahedra) observed in BeB_3[33] and in SiB_6.[34] It is interesting to note the similarity in the genesis of the 15- and the 16-vertex clusters. The fomer can be viewed as a tricapped truncated trigonal prism (3:3(3)3:3) while the icosioctahedron is, as noted above, a tetracapped truncated tetrahedron. The clusters in BeB_3 are Be_3B_{12} units where beryllium takes the three capping positions. The cluster in SiB_6 is actually $Si_{3+x}B_{12-x}$ in which three silicon atoms are capping, but some silicon is also mixed with boron on four other positions, and there are two other partially occupied silicon sites as well. Interconnected clusters are present in both phases.

Highly condensed polyhedra with the same geometry as the In_{16} cluster are found in some MM'_2 intermetallic compounds such as $MgCu_2$ and $MgZn_2$.[35-37] In these compounds (known also as "Laves phases"), the M′ atoms generate truncated tetrahedra that share all hexagonal faces, while M atoms center these and also cap the four hexagonal faces of the tetrahedra, viz., $M'_{12/6}M_{5/5}$. These condensed units are also called Friauf polyhedra and can alternatively be viewed, perhaps more simply, in terms of vertex-linked tetrahedra.

Surprisingly, individual 16-atom metal clusters with the same $\bar{4}m2$ symmetry were also recently discovered in $Y_{16}Ru_4I_{20}$.[38] Here the 16-atom yttrium polyhedra are both centered by a tetrahedron of Ru atoms and sheathed by iodine. Besides the centering, there is subtle geometric difference as well; the cluster in $Y_{16}Ru_4I_{20}$ can be considered to be the result of a tetrahedral condensation of

(27) van der Marel, C.; Braunderburg, E. P.; van der Lugt, W. *J. Phys. F: Met. Phys.* **1978**, *8*, L273.
(28) Selwood, P. W. *Magnetochemistry*, 2nd ed.; Interscience Publishers: New York, 1956; p 70.
(29) Ashcroft, N. W.; Mermin, D. N. *Solid State Physics*; Holt, Rinehart and Winston: Philadelphia, 1976; p 649.
(30) Brown, L. D.; Lipscomb, W. N. *Inorg. Chem.* **1977**, *16*, 2989.
(31) Bicerano, J.; Marynick, D. S.; Lipscomb, W. N. *Inorg. Chem.* **1978**, *17*, 2041.
(32) King, R. B. *J. Am. Chem. Soc.* **1969**, *91*, 7211.
(33) Mattes, R.; Tebbe, K. F.; Neidhard, H.; Rethfeld, H. *J. Less-Common Met.* **1976**, *47*, 29.
(34) Vlasse, M.; Slack, G. A.; Garbauskas, M.; Kasper, J. S.; Viala, J. C. *J. Solid-State Chem.* **1986**, *63*, 31.
(35) Frank, F. C.; Kasper, J. S. *Acta Crystallogr.* **1958**, *11*, 184.
(36) Muetterties, E. L.; Wright, C. M. *Q. Rev.* **1967**, *21*, 109.
(37) Hyde, B. G.; Andersson, S. *Inorganic Crystal Structures*; J. Wiley: New York, 1989; p 375.
(38) Payne, M. W.; Ebihara, M.; Corbett, J. D. *Angew. Chem., Int. Ed. Engl.* **1991**, *30*, 856.

Table III. Distances (Å) of Nearest Neighbors about Each Atom in $Na_7In_{11.76}$[a]

		In1		
In1	2.858 (3)	Na3	3.469 (2)	
In1	3.016 (3)	Na5	3.546 (7)	
In2	3.080 (3)	Na5	3.43 (1)	
In3	3.014 (3)	Na7	3.48 (1)	
In6	3.012 (2)	Na7	3.50 (1)	
In7	3.022 (2)			
		In2		
2In1	3.080 (3)	Na5	3.51 (1)	
In5	2.930 (3)	2Na6	3.34 (1)	
2In6	2.980 (2)	2Na7	3.647 (9)	
		Na8	3.45 (1)	
		In3		
2In1	3.014 (3)	Na3	3.410 (2)	
In3	2.845 (5)	2Na5	3.57 (1)	
2In7	2.985 (2)	2Na10	3.34 (1)	
In11	3.030 (5)			
		In4		
In4	3.018 (3)	Na1	3.408 (5)	
In5	3.041 (3)	Na5	3.41 (1)	
In7	2.943 (2)	Na7	3.506 (9)	
In8	2.941 (2)	Na9	3.48 (1)	
		Na9	3.71 (1)	
		Na10	3.45 (1)	
		Na11	3.49 (1)	
		In5		
In2	2.930 (3)	2Na1	3.38 (1)	
2In4	3.041 (3)	Na4	3.39 (2)	
In5	3.023 (5)	Na5	3.43 (1)	
		2Na6	3.52 (1)	
		2Na7	3.623 (9)	
		In6		
In1	3.012 (2)	Na6	3.306 (8)	
In2	2.980 (2)	Na7	3.621 (9)	
In7	3.194 (2)	Na7	3.639 (8)	
In8	2.987 (2)	Na8	3.522 (4)	
In9	3.009 (3)	Na9	3.52 (1)	
		Na11	3.262 (8)	
		In7		
In1	3.022 (2)	Na5	3.456 (7)	
In3	2.985 (2)	Na7	3.506 (9)	
In4	2.943 (2)	Na9	3.44 (1)	
In6	3.194 (2)	Na9	3.34 (1)	
In8	2.950 (2)	Na10	3.303 (6)	
In11	3.161 (3)			
		In8		
In4	2.941 (2)	Na1	3.43 (1)	
In6	2.987 (2)	Na4	3.277 (8)	
In7	2.950 (2)	Na8	3.68 (1)	
In8	2.959 (3)	Na9	3.65 (1)	
In11	3.163 (4)	Na9	3.61 (1)	
		Na11	3.347 (8)	
		In9		
In6	3.009 (3)	Na2	3.497 (2)	
In9	3.061 (4)	Na6	3.47 (1)	
In9	2.969 (3)	Na7	3.42 (1)	
In10	3.031 (3)	Na7	3.538 (9)	
In12	3.304 (2)	Na9	3.68 (1)	
In12	3.473 (4)	Na11	3.75 (1)	
		In10		
2In9	3.031 (3)	Na2	3.577 (3)	
In10	2.949 (6)	2Na9	3.62 (1)	
2In12	3.327 (3)	Na11	3.29 (1)	
		In11		
In3	3.030 (5)	Na1	3.38 (1)	
2In7	3.161 (3)	2Na9	3.36 (1)	
2In8	3.163 (4)	2Na10	3.460 (9)	
		In12		
2In9	3.304 (2)	Na1	3.06 (1)	
2In9	3.473 (4)	Na2	3.376 (3)	
2In10	3.327 (3)	Na6	3.68 (1)	
		2Na7	3.85 (1)	
		2Na9	3.90 (1)	

		Na1		
2In4	3.408 (5)	Na4	3.26 (1)	
2In5	3.38 (1)	Na6	3.61 (2)	
2In8	3.43 (1)	2Na7	3.84 (1)	
In11	3.38 (1)	2Na9	3.85 (1)	
In12	3.06 (1)			
		Na2		
8In9	3.497 (2)			
4In10	3.577 (3)			
4In12	3.376 (3)			
		Na3		
4In1	3.469 (2)	4Na5	3.75 (1)	
4In3	3.410 (2)			
		Na4		
4In4	3.524 (5)	2Na1	3.26 (1)	
2In5	3.39 (2)	Na8	3.48 (3)	
4In8	3.277 (8)			
		Na5		
2In1	3.43 (1)	Na3	3.75 (1)	
2In1	3.546 (7)	2Na7	3.68 (1)	
In2	3.51 (1)	Na10	3.45 (2)	
2In3	3.57 (1)			
2In4	3.41 (1)			
In5	3.43 (1)			
In7	3.456 (7)			
		Na6		
2In2	3.34 (1)	Na1	3.61 (2)	
2In5	3.52 (1)	Na7	3.47 (1)	
2In6	3.306 (8)	Na8	3.64 (2)	
2In9	3.47 (1)			
In12	3.68 (1)			
		Na7		
In1	3.48 (1)	Na1	3.84 (1)	
In1	3.50 (1)	Na5	3.68 (1)	
In2	3.647 (9)	Na6	3.47 (1)	
In4	3.506 (9)	Na7	3.81 (2)	
In5	3.623 (9)	Na9	3.59 (1)	
In6	3.621 (9)			
In6	3.639 (8)			
In9	3.42 (1)			
In9	3.538 (9)			
In12	3.85 (1)			
		Na8		
2In2	3.45 (1)	Na4	3.48 (3)	
4In6	3.522 (4)	2Na6	3.64 (2)	
4In8	3.68 (1)	2Na11	3.60 (1)	
		Na9		
In4	3.48 (1)	Na1	3.85 (1)	
In4	3.71 (1)	Na7	3.59 (1)	
In6	3.52 (1)	Na9	3.95 (2)	
In7	3.44 (1)	Na10	3.73 (1)	
In7	3.34 (1)	Na11	3.499 (1)	
In8	3.65 (1)			
In8	3.61 (1)			
In9	3.68 (1)			
In10	3.62 (1)			
In11	3.36 (1)			
In12	3.90 (1)			
		Na10		
2In3	3.34 (1)	Na5	3.45 (2)	
2In4	3.45 (1)	2Na9	3.73 (1)	
2In7	3.303 (6)	Na11	3.50 (2)	
In10	3.12 (1)			
2In11	3.460 (9)			
		Na11		
2In4	3.49 (1)	Na8	3.60 (1)	
2In6	3.262 (8)	2Na9	3.49 (1)	
2In8	3.347 (8)	Na10	3.50 (2)	
2In9	3.75 (1)			
In10	3.29 (1)			

[a] Limits are 3.5 Å for In–In and 3.9 Å for Na–In and Na–Na.

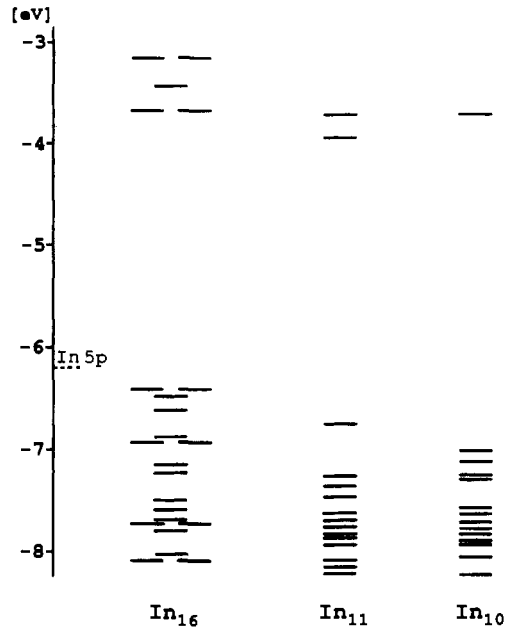

Figure 4. Extended Hückel results for the skeletal bonding levels in separate In_{16}, In_{11}, and In_{10} units in $Na_7In_{11.76}$, including exo bonds. For In_{11} and In_{16}, the highest lying one and eight of nine orbitals, respectively, are nonbonding pairs on atoms without exo In–In bonds.

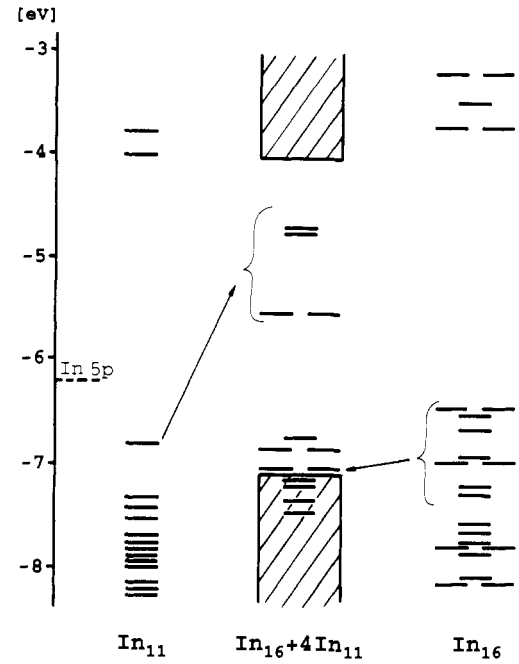

Figure 5. Perturbations on the extended Hückel results in Figure 4 when In11–In10, -12 interactions between "nonbonding" lone pairs on In_{16} and four surrounding In_{11} units are included. The explicit levels in the middle portion show only those energies that are significantly affected; the blocked areas represent the locales of unchanged skeletal bonding levels for In_{10}, In_{11}, and In_{16} in which nonbonding pairs are not important components.

four Ru-centered octahedra Y_6Ru about edges rather than as an approximately spherical deltahedron. This viewpoint follows from the fact that the yttrium atoms that cap the hexagonal faces of the truncated tetrahedron lie almost in the planes of those hexagons and thus represent smaller distortions of the starting octahedra. This condition doubtlessly relates to the presence of strong Y–Ru central forces.

Discussion in some detail of one more feature of the structure is necessary, namely, the partially occupied site of In11. The icosahedra bearing In11 (Figure 2b) are nido species, but the 63.6 (8)% occupancy of this site means that 36% of them are actually 1,3-arachno clusters. This distribution represents the upper limit for the former, judging from lattice constant variations with composition (Experimental Section). The lack of an In atom on this position does not affect the connectivity of the overall network since this is the only site in this cluster without an exo bond. Loss of an atom from this position reduces the total bonding as well as some intercluster repulsions, and less than 50% occupancy of the In11 site will decrease the number of available electrons below that evidently needed for the indium network bonding (below). Of course, fractional occupancy of some other indium sites may instead pertain at the sodium-rich limit although this does not seem indicated or necessary.

Electronic Structure. Extended Hückel MO calculations have been performed on the separate (8-bonded) *closo*-In_{16}, the (10-bonded) *nido*-In_{11} units, and the (10-bonded) *arachno*-In_{10} clusters as well as on the observed arrangement of four *nido*-(*arachno*-)In_{11} units about one In_{16} cluster, all with the observed configurations.[39] Exo bonds in cluster network are important in the bonding descriptions; therefore, dummy atoms about each species with only 5s-type orbitals were used at the positions of all exo-bonded atoms to "saturate" the exo bonding. These 5s orbitals were given Slater-type orbital exponents and energies equal to those for In 5p, although the latter quantity can in fact be that of In 5s without affecting the results significantly. Such a setup for cluster bridging is intended to make the results as close as possible to reality. Calculations on the bonding in the pairs of indium triangles (Figure 2c) showed that these each have the same electronic requirements (a'^2,e'^4) as would the component four-bonded atoms, and they were so treated thereafter. (Although 3-D band calculations would provide the ultimate results, these would be almost impossible to visualize for a calculation with 144 atoms.) The energy results for the calculations are shown in Figures 4 and 5.

(a) In_{16}. As noted earlier by Brown and Lipscomb,[30] closed polyhedra with 16, 19, and 22 atoms do not obey the $n + 1$ skeletal bonding orbital (Wade's) rule. These deviations were later generalized as "intrinsic" by Fowler.[40] Indeed, our calculations on the isolated unit show that there are 18 instead of 17 such orbitals below a 2.5-eV gap. The 36 skeletal electrons needed to fill these orbitals then put the cluster in the so-called hyperelectronic class. The earlier studies of this polyhedron only noted that an instability would be expected with $2(n + 1)$ electrons and that either $2n$ or $2n + 4$ was probable, although the one expectation of $2n$ (with boron)[30] would be quite improbable for the indium example, as the gap at that point is very small (Figure 4). Eight of the nine top bonding orbitals for this cluster shown in Figure 4 are located mainly on indium atoms that lack exo bonds (In10, -12) (the eighth orbital down is excluded). In other words, substantial p mixing is present and these filled orbitals represent combinations of outward pointing electron pairs, in contrast to dominantly s-like pairs found on atoms in the isolated cluster In_{11}^{7-} and others. Burdett and Canadell[14] showed that the highest bonding orbitals in interconnected gallium clusters are usually isolated lone pairs on atoms without exo bonds. As the nuclearity and hence the radius of the curvature of the cluster increase, they predicted that the energy of such a lone pair could become so high that it is left empty, as for that in the imaginary $B_{15}H_{14}^{3-}$ icosihexahedron. This could also lead to fractional occupancy or even expulsion of that atom. Although the present In_{16} icosioctahedron is of higher nuclearity, all lone pairs are of a bonding type. This apparent contradiction can be explained by the fact that the one lone pair in $B_{15}B_{14}^{3-}$ is surrounded by exo bonds with which it is antibonding. On the other hand, in In_{16} we have groups of four neighboring lone pairs on the top and bottom of the cluster and, although each set as a whole is antibonding with respect to the neighboring exo bonds, the lone pairs within each set are π-bonding with respect to each other. Thus, removal of one or more atoms in these sets should reduce the bonding interactions for the remaining lone pairs and raise their energies, and calculations carried

(39) Orbital parameters and energies from: Janiak, C.; Hoffmann, R. *J. Am. Chem. Soc.* **1990**, *112*, 5924.

(40) Fowler, P. W. *Polyhedron* **1985**, *4*, 2051.

out on such defect indium clusters proved this to be the case. This effect could be the reason why In(10,12) sites, although similar to the In11 site in terms of bonding, are not partially occupied.

(b) In_{11} and In_{10}. As expected, the two clusters are calculated to each have 13 skeletal bonding orbitals ($n + 2$, $n + 3$, respectively). The HOMO for In_{11} (Figure 4) is purely a lone pair on In11 that points radially from the cluster. This orbital is very much π-antibonding to the five neighboring exo bonds even though distortions at this point leave the In11 somewhat protruding. Even so, the energy gap to the next bonding orbital is nearly 0.5 eV. The HOMO calculated for the pairs of metal triangles (Figure 2c) falls at nearly the same energy, −6.9 eV.

(c) In_{16} Combined with In_{11}. Comparison of the electron counts needed and available were at this point somewhat troublesome. However, in connection with the nonstoichiometry, we noticed that the distances from In11 in each nido iscosahedron to In12 (3.872 (6) Å) and to two In10 atoms (4.099 (5) Å) in the In_{16} cluster appeared to afford some significant repulsive interactions between these atoms relative to distances already considered as "bonding" in the individual units, 2.9–3.5 Å. One example of these repulsive contacts is represented by the dashed lines in Figure 1. Each In11 atom approximately caps a triangular face formed by the In10 and two In12 atoms in the nearest icosioctahedron, so that the former's lone pair lies almost normal to that face, while the lone pairs on In10 and In12 are directed radially outward from the In_{16} cluster. This arrangement suggests that interactions between these orbitals are important. Extended Hückel MO calculations were therefore performed on the collection of an In_{16} cluster surrounded by one, two, three, or four *nido*-In_{11} clusters[41] (the differences from four in each case were taken to be the number of noninteracting *arachno*-In_{10} clusters). The noteworthy result is that the lone pair orbitals on all In11 atoms are in the process pushed up in energy by ca. 1.65 eV and thus become antibonding and empty and the LUMO for the macrocluster. The highest bonding orbitals on In_{16} are correspondingly lowered by this effect. The important consequences of these intercluster interactions are shown in Figure 5 where only the altered levels are shown in the middle portion, the blocks representing intracluster levels that are basically unchanged by these effects. The HOMO–LUMO gap for the macrocluster is now approximately 1.2 eV, although this detail clearly depends on orbital parameters utilized.

Electron Count. The compound is now very slightly electron-rich judging from the numbers of electrons needed and available. We count the electrons in the following way. Each unit cell contains 2 icosioctahedra, 8 icosahedra (which round off to 5 nido and 3 arachno), and 24 isolated, four-bonded indium atoms. The electron requirement of each unit and the total for a closed-shell system are

	skeletal	exo	lone pair	Σ	total
$2In_{16}$	36	8	16	60	120
$5In_{11}$	26	10	0	36	180
$3In_{10}$	26	10	0	36	108
$24In_1$				4	96
closed-shell sum					504
available (141 × 3 + 84 × 1)					507
difference					+3

The unit cell contains 141 indium atoms (with $^5/_8$th occupancy of In11) that provide three valence electrons each, and the 84 sodium atoms furnish one electron each. The total is 507 available electrons per cell, 3 (0.6%) more than necessary for closed shells for all species. A 50% occupancy of In_{11} with all other atoms fixed would close the sum and give a Zintl phase. The above result is changed insignificantly (0.2e) if the refined occupancy (63.6 (8)%) is used instead of approximated as 62.5%. Of course, there are other ways to account for and to express this evident electron surplus in the solid state. It is very encouraging to note the strong support provided to the bonding model by the measured metallic conductivity and the Pauli-like magnetic susceptibility (above).

The effects of the nonstoichiometry observed on the sodium-rich, or indium-poor, side of the composition studied structurally are also completely consonant with the above picture. One way to accomplish such a composition change would be to add more sodium ions to the cell, but this would seem to be inconsistent with the significant (0.4%) *contraction* of c. The last instead appears to be clearly associated with the unique In11 and its significantly short "nonbonding" distances to In12 and In10 in the In_{16} cluster since their result is directed along $\vec{c}$. Although we cannot tell the amount, additional atoms are evidently removed from the In11 site preferentially in sodium-richer systems.

The bottom line in our assessment of the structure of and bonding in $Na_7In_{11.76}$ at the indium-rich limit is that the valence electron count lies only very slightly above that necessary to give a closed-shell configuration to the individual units. This in itself is quite satisfying; a structure of this complexity must have quite specific electronic requirements. The character of the excess electron distribution cannot be better defined at this time. Figure 5 represents the situation only at $k = 0$, although it does not seem likely that the relatively large gap at Γ will be bridged elsewhere in k space. Whether the excess electrons lie in the conduction band implied by the figures or in states with a substantial sodium component (as in K_8In_{11} apparently) is not known, although there are many Na–Na separations that are less than that in the bcc metal (3.72 Å). In a broader sense, $Na_7In_{11.76}$ seems to be another example of a "metallic Zintl phase"[42] in which the small perturbations at E_F (sea level) that make it (weakly) metallic scarcely obscure the strong covalent bonding associated with the network and the clusters at lower energies (in the depths of the sea—see Nesper[42]). The structure itself represents the best ordered solution to a complex problem of filling space with cations and cluster anions as well as the requirements of cluster stability and size and the need for some intercluster bonding. The variety of clusters and structures found for indium and for gallium illustrate well the considerable number of possibilities available in these systems.

We should again reemphasize that the exo bonding of the clusters of indium and gallium is the major route by which what would otherwise be isolated ions with a high charge, e.g., In_{16}^{20-}, achieve smaller and more reasonable values. The "inert s pair" is in effect changed into a bonding role in the process, reducing the charge by one for each such bond. This means is already known to be dominant in polygallium chemistry, and what we have seen of indium systems so far indicates a parallel yet very distinctive cluster chemistry with perhaps fewer nonstoichiometry complexities and more simple ions.

The Na–In system alone illustrates a considerable variety. In addition to $Na_7In_{11.8}$ (37.3 at. % Na), the slightly indium-richer $Na_{15}In_{28}$ (34.9%), apparently the last binary compound in this direction, exhibits very similar building blocks and structural array: 10-bonded *nido*-In_{11}, 12-bonded (not 8) *closo*-In_{16}, and similar triangles of isolated atoms. The indium-richer phases appear to be only NaIn, isostructural with "the" Zintl phase NaTl (stuffed diamond), and Na_2In which contained isolated indium tetrahedra, nominally In_4^{8-} and isoelectronic with Sb_4, etc.[16] Subtle details of crystal packing appear to be responsible for the occurrence of another isolated cluster, the hypoelectronic In_{11}^{7-} (D_{3h}), in a phase A_8In_{11} with 42.1% A only for potassium or a limited amount of rubidium. More details on this unusual indium chemistry will follow.

Acknowledgment. We are indebted to J. Shinar for the use of the Q apparatus, to J. E. Ostenson for the magnetic data, and to G. J. Miller for suggestions on some of the calculations.

Supplementary Material Available: Tables of data collection and refinement details and anisotropic displacement parameters for $Na_7In_{11.76}$ (2 pages); a listing of structure factor data for the same compound (10 pages). Ordering information is given on any current masthead page.

(41) The calculation for $In_{16} + 4In_{11}$ actually exceeded the capacity of the program, and so the essential portion, the four In11 atoms, was represented by adjusted 5s orbitals on four isolated atoms. But the results with fewer In_{11} units make it clear that the In11 interactions are quite independent, especially those at opposite ends of the In_{16} cluster.

(42) Nesper, R. *Prog. Solid State Chem.* **1990**, *20*, 1.